Click Here for Full Article

A new polar magnetic index of geomagnetic activity

Wladislaw Lyatsky[1,2] and George V. Khazanov[1]

Received 20 December 2007; revised 21 February 2008; accepted 5 April 2008; published 28 June 2008.

[1] We developed a new polar magnetic (*PM*) index of geomagnetic activity which, similarly to the existing polar cap index, was computed from magnetic field data from near-pole geomagnetic observatories. However, we used a different method for its calculation, which provided the high correlation of this index with both solar wind data and many events in geospace environment. This improves significantly the reliability of forecasting geomagnetic disturbances and such key parameters as cross-polar-cap voltage and Joule heating in high-latitude ionosphere, which play an important role in the development of global geomagnetic, ionospheric, and thermospheric disturbances. In this paper, we examined *PM* index in the Northern Hemisphere only. We tested the *PM* index for 10-year period. The correlation between *PM* index and upstream solar wind data for all these years is very high (the squared correlation coefficient $R^2 \approx 0.74$ which corresponds to the linear correlation coefficients $R \approx 0.86$). The *PM* index also shows the high correlation with the cross-polar-cap voltage and hemispheric Joule heating (the squared correlation coefficient R^2 between the actual and predicted values of these parameters reaches $\sim$0.81 which corresponds to the linear correlation coefficients $R \approx 0.9$), which results in significant increasing the prediction reliability of these parameters. Thus, the polar magnetic (*PM*) index of geomagnetic activity provides a significant increase in the forecasting reliability of geomagnetic disturbances and related events in geospace environment, and it may be used as an important input parameter in modeling ionospheric, magnetospheric, and thermospheric processes.

Citation: Lyatsky, W., and G. V. Khazanov (2008), A new polar magnetic index of geomagnetic activity, *Space Weather*, *6*, S06002, doi:10.1029/2007SW000382.

1. Introduction

[2] Geomagnetic activity indices are used for measuring the level of geomagnetic activity. These indices are calculated from measurements of geomagnetic disturbances at specific geomagnetic observatories. Various indices show different types of geomagnetic activity [e.g., *Rostoker*, 1972; *Mayaud*, 1980]. The auroral electrojet *AL* and *AE* indices show geomagnetic activity in the auroral zone related to substorm activity. The *Kp* index shows geomagnetic activity at middle latitudes. The low-latitude *Dst* index shows the intensity of the ring current, produced by energetic particles in the magnetosphere. The polar cap *PC* index [*Troshichev et al.*, 2006] measures geomagnetic activity, produced by overhead ionospheric currents and field-aligned currents, in north and south polar caps. Since the primarily source of geomagnetic disturbances is the solar wind, geomagnetic activity indices show the clear correlation with upstream solar wind/IMF data.

[3] The existing geomagnetic activity indices were developed many years ago, when our knowledge on the magnetosphere and ionosphere was insufficient, and improving the reliability of space weather prediction requires the development of more appropriate indices. The basic requirements to such indices are the following: They should (1) have a better and more stable correlation with upstream solar wind/IMF data, (2) have good correlation with key ionospheric and magnetospheric parameters (such as cross-polar-cap potential drop, Joule heating, and others, which used as input parameters for modeling the processes in the magnetosphere, ionosphere, and thermosphere), and (3) be available in near-real time.

[4] The purpose of this paper is to develop an index of geomagnetic activity, which responds to the requirements mentioned above. We call this index the polar magnetic (*PM*) index. This index was computed from magnetic field measurements from two near-pole geomagnetic observatories, Thule (Greenland) and Vostok (Antarctica), the same observatories that are used for deriving the existing polar cap (*PC*) index, but we used a different method for computing the *PM* index. The *PM*

[1]Space Plasma Group, NASA Marshall Space Flight Center, Huntsville, Alabama, USA.
[2]Also at Oak Ridge Associated Universities, Oak Ridge, Tennessee, USA.

Copyright 2008 by the American Geophysical Union

index shows much better correlation with solar wind coupling function and related events than other existing indices, including *PC* index. Although we computed *PM* index from both observatories in two hemispheres, however, the data from the Vostok observatory are only partially available for the interval (1995–2004) considered, and in the present paper we consider results obtained only from the Thule observatory.

2. Method of Calculation of the Polar Magnetic Index and Data Used for Analysis

[5] As mentioned above, the *PM* index, similarly to the existing polar cap (*PC*) index, was computed from ground magnetic field measurements from near-pole geomagnetic observatories. The polar cap *PC* index was introduced by *Troshichev et al.* [2006] for measuring the magnetic effect of the transpolar equivalent ionospheric current flowing across the polar cap. It was suggested that this current is proportional to the dawn-to-dusk ionospheric convection flow, which is responsible for the generation of global geomagnetic activity and related events. The transpolar equivalent ionospheric current points commonly between noon and dawn, so that the vector of magnetic disturbances on the ground points somewhere between noon and dusk. For deriving the *PC* index, the component of magnetic disturbances, H', across a statistically average direction of the transpolar electric current is computed:

$$H' = H \cdot \frac{J_{tr} \times e_z}{|J_{tr}|} \tag{1}$$

where H' is the magnitude of a geomagnetic disturbance in the horizontal plane across the average ionospheric transpolar current, J_{tr}; H is the vector of a geomagnetic disturbance in the horizontal plane, and e_z is the unit vector along the ambient geomagnetic field that is assumed to be directed along the z axis. The "true" direction of the transpolar current is found from the condition that the H' values show the best correlation with upstream solar wind/IMF data.

[6] Thus, the method used for computing the *PC* index is based on suggestion that only the transpolar current component along its average direction (which may be different for different UT and season) is responsible for global geomagnetic activity. Formula (1) for computing *PC* index suggests that the transpolar current, flowing across a statistically average direction of this current, produces no geomagnetic activity. We found, however, this approach underestimates the level of global geomagnetic activity, predicted from *PC* index, since the transpolar equivalent ionospheric current contributes to geomagnetic activity even when it is significantly deflected from its average direction. Therefore, we used another approach and derived a new geomagnetic activity index, which accounts for the effect of the transpolar ionospheric current on global geomagnetic activity even when this current is significantly deflected from its average direction.

[7] For calculation of the polar magnetic (*PM*) index, we used the Akasofu function [*Perreault and Akasofu*, 1978; *Akasofu*, 1981; see also *Lyatsky et al.*, 2007, and references therein]

$$F_A \sim B_\perp \sin^\nu(\theta/2) \tag{2}$$

which was introduced to improve the correlation between the interplanetary magnetic field (IMF) and geomagnetic activity indices. In this formula, $B_\perp$ is the IMF vector in the y-z plane in the solar-magnetospheric frame, θ is the angle between the z (northward) axis and the direction of $B_\perp$ in the y-z plane, and ν is the power. The Akasofu function derives the effectiveness of reconnection at dayside magnetopause when IMF vector may be significantly deflected from the z-axis. This makes the problem similar to our case.

[8] For deriving *PM* index, we introduced a function, similar to the Akasofu function, and applied it to ground geomagnetic disturbances

$$\Delta H = H_\perp \sin^\nu(\varphi/2) \tag{3}$$

where $H_\perp$ is a total geomagnetic disturbance in the polar cap region in the horizontal plane, φ is the angle measured from the direction, opposite to the transpolar current, to its actual direction, and the power, ν, is derived from experimental data to provide the best correlation between ΔH and upstream solar wind/IMF data, which gives $\nu \approx 3$. The angle φ is derived from experimental data for each UT hour and season. If the transpolar current is along its averaged direction, we have $\varphi = \pi$. In this case, (3) coincides with (1).

[9] The ΔH quantities, derived by (3), may be significantly different from H' in (1), which is used for calculating the *PC* index. For instance, if the transpolar current is deflected from its average direction by the angle of $\pi/2$, from (1) we obtain $H' = 0$, while from (3) we obtain $\Delta H \approx 0.35\, H_\perp$, that is, even in this case the contribution from the transpolar current to ΔH, accordingly to (3), remains very significant.

[10] Substituting the power $\nu = 3$, the quantity ΔH may also be rewritten

$$\Delta H = H_\perp \sin^3(\varphi/2) = H_\perp \sin^3[0.5\ \mathrm{acos}(-H'/H_\perp)] \tag{4}$$

This expression may be used for a rough estimate of *PM* . index. The correlation with upstream solar wind/IMF data, however, is better while accounting also for the magnetic field vertical H_z component. Then the finale formula for deriving the *PM* index becomes the following

$$PM = \left(H_\perp \sin^3[0.5\ \mathrm{acos}(-H'/H_\perp)] + 0.25|H_z|\right) f(UT, \mathrm{season}) \tag{5}$$

where the factor 0.25 is found to provide the best correlation of the resulting *PM* index with upstream solar wind/IMF data, and *f* (*UT*, season) is a function, reducing the effect of *UT* and season, which are very strong at high latitudes [*Cliver et al.*, 2000; *Lyatsky et al.*, 2001].

[11] For calculation of *PM* index, we used the x, y, z coordinate system, where in the Northern Hemisphere the axis x is northward, axis y is eastward, and axis z is downward. We removed geomagnetic disturbances related to the sign (but not the absolute value) of the interplanetary magnetic field IMF *By*, which are related to the so-called Svalgaard-Mansurov effect [*Mansurov*, 1981; *Svalgaard*, 1973]. This effect is associated with a single current vortex located in the polar cap and changing its direction with the sign of IMF *By*. This current does not contribute to the total transpolar current but produces a significant spread in the correlation between computed ΔH fields and upstream solar wind data. We removed also the secular and quiet-day diurnal variations of the magnetic field, and reduced the *UT*/season variations. To reduce the *UT*/season variations, we used a simple analytical formula $A = A_0\, f\,(UT,\ \text{season})$ where A_0 are an actually measured magnetic field, A is a corrected magnetic field, and $f\,(UT,\ \text{season})$ is

$$f(UT, \text{season}) = 1 - 0.3\cos[2\pi(D - 174)/365] - 0.5\cos[2\pi(UT - 15.5)/24] \qquad (6)$$

where D is the day of year and UT is measured in hours.

[12] To account for the *UT*/seasonal variation of the average direction of the transpolar current and H' field for computing the H' field, we used the expression

$$H' = X\cos[2\pi(UT - g)/24] + Y\sin[2\pi(UT - g)/24] \qquad (7)$$

where X and Y are the corrected magnetic field disturbances along the x (northward) and y (eastward) axes, UT is universal time in hours, and g is a corrective function of season and UT which was derived from experimental data. We found the g function from the expression:

$$g = 7.2 + 0.5\cos[2\pi(D - 174)/365] - 0.12\cos[2\pi(UT - 11.5)/24] \qquad (8)$$

The coefficients in (8) were derived to provide the best correlation between the *PM* index and upstream solar wind/IMF data.

[13] Thus, as mentioned above, using only the H' magnetic field component in (1) for deriving the *PC* index provides underrating the real cross-polar-cap convection flow and transpolar current, responsible for global geomagnetic activity, due to significant deflections of the convection flow and the transpolar current from their average directions. It is interesting to mention in this connection that *Ballatore and Maclennan* [1999] reported many cases when significant geomagnetic activity, observed near the polar cap boundary, was related to a very low *PC* index. The method that we used for deriving the polar magnetic *PM* index is accounting for possible deflections of the transpolar current and related magnetic field in the polar cap from their average directions. This method provides a more correct evaluation of the transpolar current, responsible for global geomagnetic activity not only in the polar cap but also at middle and lower latitudes.

[14] The correlation between *PM* index and F^* coupling function is better than that between H'/PC and F^* function for each years from 1995 through 2004, and goodness of fit, R^2, varies from ~0.8 (near solar minimum) to ~0.7 (near solar maximum) which corresponds to the variation of the correlation coefficient, R, from ~0.9 to ~0.84. Additionally to the high correlation with upstream solar wind/IMF data, the *PM* index shows also high correlation with key parameters in the magnetosphere and ionosphere such as *AL* and *Kp* indices, cross-polar-cap potential drop, and Joule heating released in high-latitude ionosphere. These effects will be considered in the next sections.

[15] For computing the polar magnetic (*PM*) index, we used hourly measurements from high-latitude Thule (corrected geomagnetic latitude $\Lambda \approx 85°$) and Vostok ($\Lambda \approx -83°$) observatories in Northern and Southern Hemispheres, respectively, for 10 (1995–2004) years. Although we computed *PM* index in both polar caps, here we are presenting the results obtained for the Northern Hemisphere only (the magnetic field measurements from Southern Hemisphere are not available for all years). We took the magnetic field data and geomagnetic activity indices from the World Data Centers in Kyoto, Japan, and Denmark (Danish Meteorological Institute) at Web sites http://swdcwww.kugi.kyoto-u.ac.jp and http://web.dmi.dk, respectively. We also used the hourly upstream solar wind/IMF data, available from the Goddard Space Flight Center Web site at ftp://nssdcftp.gsfc.nasa.gov/spacecraft_data/omni/.

3. Coupling Function

3.1. Deriving the Appropriate Coupling Function

[16] To improve the effectiveness of forecasting geomagnetic activity, it is necessary to choose also an appropriate solar wind-geomagnetic activity coupling function, which is a combination of solar wind/IMF parameters providing the best fit with geomagnetic activity. Most important factors responsible for geomagnetic activity, are the solar wind speed V and the IMF B_z component in solar-magnetospheric coordinate system. Additional parameters, responsible for geomagnetic activity, are the IMF azimuthal component (IMF B_y) and solar wind density (or pressure).

[17] Mostly known coupling functions are the product of the solar wind speed, V, and IMF B_z,

$$F_{V\cdot Bz} \sim V \cdot B_z \qquad (9)$$

and the Akasofu coupling function [*Perreault and Akasofu*, 1978; *Akasofu*, 1981]

$$F_{Akasofu} \sim VB_{yz}^2 \sin^4(\theta/2) \tag{10}$$

where B_{yz} is the IMF vector in the y-z plane and θ is the clock angle between the z (northward) axis and the $\boldsymbol{B}_{yz}$ vector. The Akasofu function was introduced to measure the energy flux from the solar wind to the magnetosphere. Therefore, for the correlation of upstream solar wind/IMF data with ground magnetic or electric fields, some modifications of the Akasofu function are commonly used, for instance, the Kan-Lee coupling function [*Kan and Lee*, 1979]

$$F_{Kan\text{-}Lee} \sim VB_{yz} \sin^2(\theta/2) \tag{11}$$

These coupling functions show a relatively good correlation for some time intervals but fail for other intervals. *Lyatsky et al.* [2007] proposed a coupling function, obtained from a simple theoretical consideration and linking upstream solar wind data to geomagnetic activity. They used the Perreault-Akasofu method [*Perreault and Akasofu*, 1978] and took into account a scaling factor due to polar cap expansion while increasing a reconnected magnetic flux in the dayside magnetosphere. The coupling function obtained shows good correlation with geomagnetic activity indices but is dependent on solar cycle. For moderate and high solar activity, the coupling function may be written in the following form:

$$F_\alpha = aVB_{yz}^{1/2} \sin^2(\theta/2) \tag{12}$$

where a is a coefficient. For solar minimum, the best correlation with geomagnetic activity takes place for coupling function F_α^γ where $\gamma \approx 1.4$. If V is measured in km/s and B_{yz} in nT, the coefficient a = 0.01. The F_α coupling function is different from coupling functions, used earlier, mainly by the power of B_{yz}, which is a result of the conservation of reconnected magnetic flux. This coupling function shows an effective ionospheric electric field in the region of open (reconnected) field lines computed with accounting for the scaling factor.

[18] The F_α coupling function may be improved while accounting for the effect of solar wind pressure/viscosity on geomagnetic activity. This effect was discussed earlier by many researchers [e.g., *Tsurutani and Gonzalez*, 1995]. We used a coupling function:

$$F = F_\alpha + F_{visc} \tag{13}$$

where the term F_{visc} = b $n^{1/4}$ $V^{3/2}$ is accounting for a contribution from viscous interaction of the solar wind with the geomagnetic field that becomes especially significant for small or northward IMF (e.g., *Tsurutani and Gonzalez* [1995] reported that the viscosity contribute up to 10% to summary convection while *Borovsky and Funsten* [2003] found this contribution to be up to 20%). The formula for F_{visc} has been derived from dimensional arguments, which leads to $F_{visc} \sim n^{1/4} V^{3/2}$. If the solar wind speed V, the IMF, and solar wind number density n are measured in km/s, nT, and cm^{-3}, respectively, the coefficients a = 0.01 and $b \approx 2 \times 10^{-4}$. The F coupling function means an ''effective'' electric field in the polar ionosphere, measured in mV/m.

[19] The coupling function (13) shows better correlation with geomagnetic activity indices than the coupling function (12) does. However, it does not eliminate yet the dependence on solar cycle. We found that the solar cycle effect may be significantly reduced while using a dimensionless coupling function:

$$F^* = cF^2/(F + C)^2 \tag{14}$$

where F is derived by (13), the factor c is chosen equal to 100 (for convenience), and the factor C = 26 was derived from experimental data to provide the best fit correlation of the F* function with *PM* and *PC* geomagnetic activity indices. The F* coupling function is convenient and it provides very good correlation with geomagnetic activity for any levels of solar and geomagnetic activity as demonstrated in the next section. In this study, we will used this dimensionless F* coupling function. We note that the correct choice of the coupling function is very important for improving the correlation of upstream solar wind parameters with geomagnetic activity indices and related events in the Earth's magnetosphere and ionosphere.

3.2. Correlation of *PM* and *PC* Indices With Upstream Solar Wind/IMF Data

[20] As mentioned above, the main difference between the polar magnetic (*PM*) index and the existing *PC* index is that the polar magnetic (*PM*) index is accounting for the contribution from the transpolar current to geomagnetic activity even when the transpolar current is significantly deviated from its average direction. We will show that this leads to a strong increase in the correlation between the *PM* index and upstream solar wind/IMF data.

[21] For this analysis, we took hourly mean values of *PM* and *PC* indices and upstream solar wind/IMF data; the latter were shifted in time to the magnetospheric bow shock position. For computing the coupling function, we used the OMNI data set, which includes the measurements of upstream solar wind/IMF data measured with the Wind or ACE satellites. Since the responses in geomagnetic activity delay on average for ~0.5 h relatively to variations in the solar wind [e.g., *Lyatsky et al.*, 2006], we compared geomagnetic indices, computed for the time ''t,'' with the F coupling function, related to the time (t − 0.5 h), which was approximately derived as 0.5[$F(t)$ + $F(t - 1\text{ h})$].

[22] The correlation of the *PM*/*PC* indices with the $V \cdot B_z$ coupling function is commonly worse than that with other coupling functions. For instance, the squared correlation

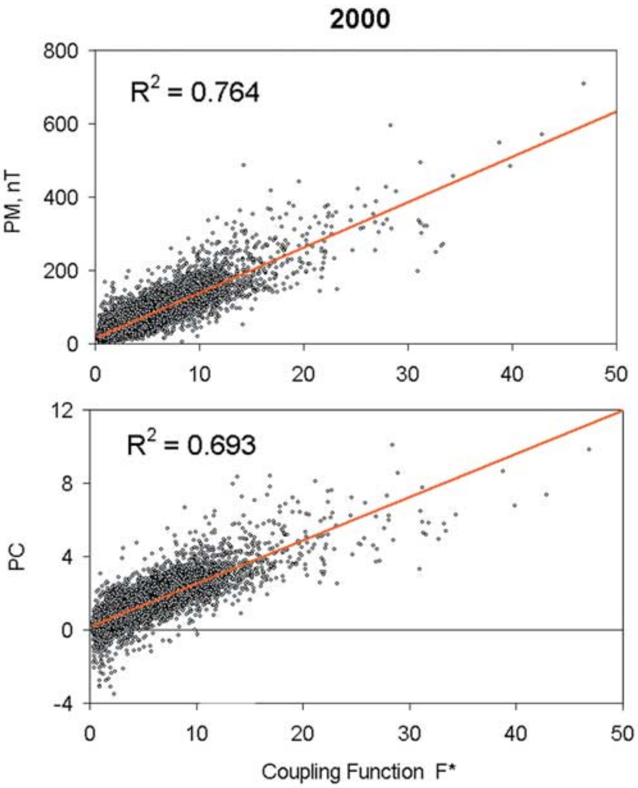

Figure 1. An example of the correlation between *PM*/*PC* indices and the dimensionless F^* coupling function for 2000.

coefficient, R^2, for the correlation between *PM*/*PC* indices and $V \cdot B_z$ is $\sim$0.4–0.5. The correlation of *PM* and *PC* indices with other coupling functions, mentioned above, and especially with the dimensionless F^* coupling function, derived by (14), is better.

[23] Figure 1 shows an example of the correlation between *PM*/*PC* indices and the F^* coupling function for 2000, related to high solar activity. One can see that the correlation between *PM* index and F^* coupling function is significantly better than that between *PC* index and the same F^* function.

[24] Figure 2 shows the dependence of goodness of fit (R^2) of the correlation between *PM*, *PC*, and *AL* indices and the F^* coupling function for the period of 10 years (from 1995 through 2004). To reduce the strong year-to-year variations, the values of R^2 in this figure were averaged for 3 years. The *PM* index shows the better correlation for all years than two other indices. The goodness of fit, R^2, for *PM* versus F^* function varies from $\sim$0.77 for solar minimum to $\sim$0.7 for solar maximum, which corresponds to the variation of the linear correlation coefficient, R, from $\sim$0.88 to $\sim$0.84, respectively. For *PC* and *AL* indices, R^2 varies in a similar way but is less in magnitude. The correlation between *PM* index and F^* coupling function in Figure 2 is significantly higher than that for two other indices for all years considered.

4. Seasonal and UT Variations in Correlation Between *PM*/*PC* Indices and Upstream Solar Wind/IMF Data

[25] The existing polar cap *PC* index has a strong UT/season dependence in its correlation with solar wind/IMF data. In contrast to that, the correlation of the *PM* index with F^* coupling function shows a weak UT/season dependence. This interesting feature is shown in Figures 3 and 4.

[26] Figure 3 is similar to Figure 2 but related to four summer (May–August) months in the Northern Hemisphere. We remind that in this paper we used the *PM*, *PC*, and *AL* indices only for the Northern Hemisphere. Figure 3 shows the dependence of goodness of fit (R^2) of the correlation of *PM*, *PC*, and *AL* indices with the F^* coupling function for the period of 10 years. To reduce strong year-to-year spread of points in this figure, the values of R^2 were averaged for 3 years. This does not affect the average magnitude of correlation coefficients but makes the curves to be better separated in Figure 3. We note that for local winter the difference in the correlation of these indices with coupling function is not as strong as for local summer. Figure 3 demonstrates the dramatic drops in the correlation of *PC* and *AL* indices with F^* function in the summer months, which are especially strong in years of high solar activity, while the correlation *PM* index with F^* coupling function varies insignificantly and the squared correlation coefficient, R^2,

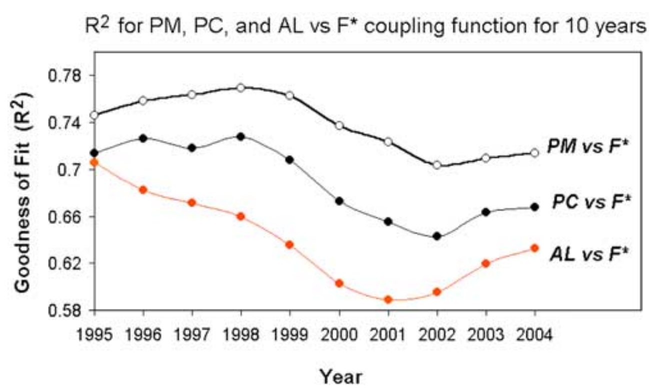

Figure 2. Solar cycle variation in the correlation. Goodness of fit (R^2) of the correlation of *PM*, *PC*, and *AL* indices with F^* coupling function is shown for 10 years (1995–2004). The values of R^2 are averages for 3 years. The correlation coefficients among hourly means for the *PM* versus F^* (empty circles), *PC* versus F^* (black circles), and *AL* versus F^* (red circles) are shown at the center of the 3-year range of data to which they refer.

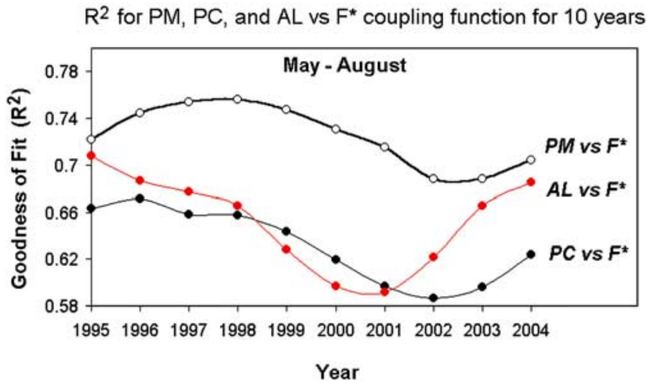

Figure 3. Summer drop in the correlation. This figure is similar to Figure 2 but related to summer months (May – August) only for 1995 – 2004. Goodness of fit (R^2) of the correlation of *PM*, *PC*, and *AL* indices with F^* coupling function is shown. For better separation of the curves in this figure, the values of R^2 were averaged for 3 years and are shown at the center of the 3-year interval to which they refer.

remains at the level of ~0.7 that corresponds to the linear correlation coefficient $R \approx 0.84$.

[27] Figure 4 shows goodness of fit (R^2) of the correlation between *PM*/*PC* indices and F^* coupling function as a function of universal time for the same 10 years. Figure 4 (left) is related to low and moderate solar activity while Figure 4 (right) is related to high solar activity. Black circles show goodness of fit, R^2, for *PM* versus F^* function for each year while red circles show R^2 for *PC* versus F^*. The correlations of *PM* and *PC* indices with F^* coupling function are close in the interval of ~2200 – 0400 UT but strongly different in the interval of 1000 – 2000 UT.

5. Correlation With *AL* and *Kp* Indices

[28] In this section we will consider the correlation between the *PM* index and the other two indices of geomagnetic activity: the *AL* and *Kp* indices. The auroral electrojet *AL* index is derived from measuring the negative (southward in the Northern Hemisphere) variations in the geomagnetic field horizontal component at 12 geomagnetic observatories spread along an average position of the auroral zone. This index shows substorm activity in the auroral zone, which contributes significantly (through the substorm-related field-aligned currents) to the magnetic field in the polar cap [e.g., *Huang*, 2005; *Lyatsky et al.*, 2006].

[29] Figure 5 shows goodness of fit (R^2) of the correlations of *PM* and *PC* indices with *AL* index for 1995 – 2004. Since *AL* index is not available for the year 1996, we computed an expected magnitude of R^2 for *PM* and *PC* indices versus *AL* index for this year by interpolating between the magnitudes of R^2 for the years 1995 and 1997. The correlation between *PM* and *AL* indices is remarkably better than that between *PC* and *AL* indices for all years considered.

[30] A considerable drop in the correlation of *PM* and *PC* indices with *AL* index for years near the solar maximum in Figure 5 may be caused by the expansion of the auroral oval during strong geomagnetic disturbances, which occur more frequently during high solar activity. The expanded auroral oval may be shifted equatorward of the position of geophysical observatories, responsible for computing the *AL* index [e.g., *Rostoker*, 1972]. In such cases, the *PM* index, computed from magnetic field variations from both overhead ionospheric currents and remote field-aligned cur-

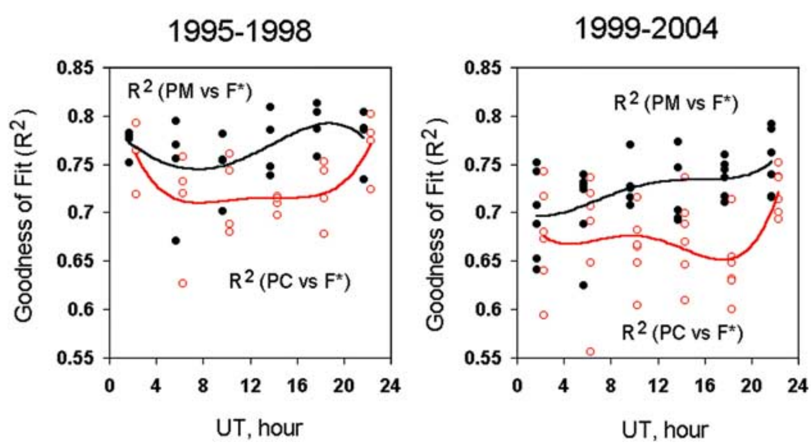

Figure 4. UT variation in the correlation of *PM*/*PC* indices with F^* coupling function. Shown are the yearly mean values of R^2 for 4-h UT intervals for the years shown above the figure, so that each circle in this figure refers to 1-year value of R^2. Black circles are related to *PM* index while open red circles to *PC* index, and these circles are shown at the center of the 4-h intervals to which they refer. Shown are (left) low and moderate activity (1995 – 1998) and (right) high activity (1999 – 2004). The curves are the fourth-order polynomial fit to the data.

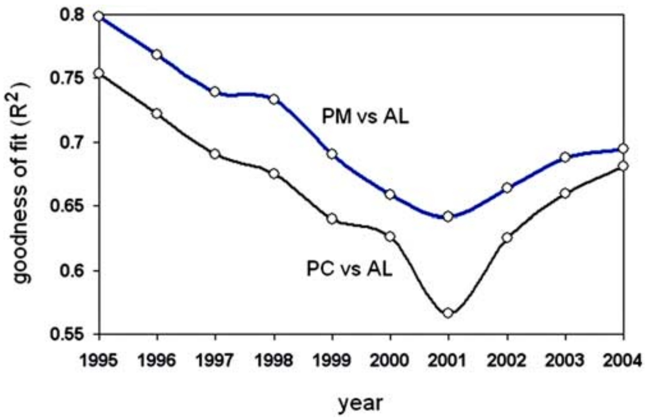

Figure 5. Correlation between *PM*/*PC* indices and *AL* index. Goodness of fit (R^2) of the correlation of *AL* index with *PM* and *PC* indices for 1995–2004.

rents, may provide more reliable information on the auroral electrojet than *AL* index does.

[31] Another important geomagnetic index, the *Kp* index, shows geomagnetic activity at subauroral and middle latitudes. This index is widely used as the input parameter for modeling magnetospheric and ionospheric processes. We note that *Kp* index is a nonlinear function of geomagnetic activity, and while comparing it with other indices, the best correlation takes place not with *Kp* index but with $Kp^{1.5}$.

[32] Figure 6 shows the goodness of fit (R^2) of the correlation of *PM*, *AL*, and *PC* indices with $Kp^{1.5}$ for 1995–2004. One can see that the correlation between *PM* and $Kp^{1.5}$ is significantly better than that for other two indices. To reduce the strong year-to-year variations in the correlation between these indices, the yearly mean values of R^2 were averaged for 3 years to smooth the curves in Figure 6. Figure 6 demonstrates once again that the *PM* index is more appropriate for the measurement of global geomagnetic activity than other existing indices do.

6. Correlation With Cross-Polar-Cap Potential Drop and Joule Heating

[33] The cross-polar-cap voltage and Joule heating of high-latitude ionosphere are two key parameters, which used for modeling the magnetosphere, ionosphere, and thermosphere [e.g., *Richmond and Kamide*, 1988; *Khazanov et al.*, 2003; *Weimer*, 2005; *McHarg et al.*, 2005; *Knipp et al.*, 2004]. The cross-polar-cap (CPC) voltage shows an electric energy flux entering the dayside ionosphere from the solar wind, while hemispheric Joule heating shows an energy flux spending on heating of neutral atmosphere. Joule heating (*JH*) produces the expansion of upper atmosphere that affects thermospheric dynamics and satellite orbits.

[34] We will show that the *PM* index may be successfully used for reliable monitoring these parameters. For the analysis, we used hourly mean values of the CPC voltage and Joule heating for 1998, computed with the Assimilative Mapping of Ionospheric Electrodynamics (AMIE) technique [*Richmond and Kamide*, 1988; *Lu et al.*, 1995; *Ridley and Kihn*, 2004], which were kindly provided by A. Ridley of University of Michigan. The AMIE technique is widely suggested to be one of the best methods for deriving the CPC voltage and Joule heating. Since this technique requires assimilation of data from a large number of geomagnetic observatories, modeling results are not available in a real time. Therefore, monitoring the CPC voltage and Joule heating in near-real time remains an important problem [*Chun et al.*, 1999, 2002; *McHarg et al.*, 2005].

[35] Figure 7 shows the correlation of hourly values of the AMIE cross-polar-cap potential drop, *U* (kV), with *PM* and *PC* indices for all days of 1998. One can see that the correlation between *U* (kV) and *PM* index is much better ($R^2 \approx 0.78$) than that between *U* (kV) and *PC* index ($R^2 \approx 0.69$).

[36] Figure 8 shows the correlation of hourly values of the root square of the AMIE total hemispheric Joule heating, *JH*, with *PM* and *PC* indices for all days of 1998. The correlation for $JH^{1/2}$ versus *PM* index ($R^2 \approx 0.75$) is also much better than that versus *PC* index ($R^2 \approx 0.68$).

[37] The correlation may be even more precise by using not only *PM* index but also upstream solar wind/IMF data (the F^* coupling function). The comparison of predicted and "actual" (AMIE) values of the cross-polar-cap voltage and Joule heating is presented in Figure 9, which shows the correlation between these quantities for all days of 1998. This figure shows very high correlation between the predicted and "actual" AMIE values (the squared correlation coefficient $R^2 \approx 0.81-0.82$ that corresponds to the linear correlation coefficient $R \approx 0.9$) for both *U* voltage

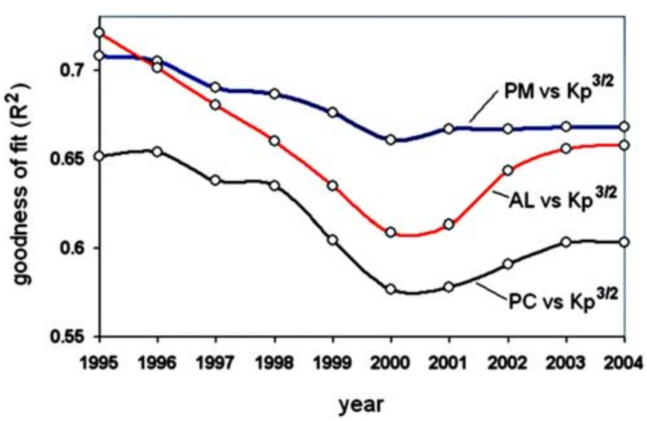

Figure 6. Goodness of fit (R^2) of the correlation of $Kp^{1.5}$ with *PM*, *AL*, and *PC* indices for 1995–2004. The correlation between $Kp^{1.5}$ and *PM* is significantly better than that for other two indices. Presented values of R^2 are averages for 3 years and are shown at the center of the 3-year interval to which they refer.

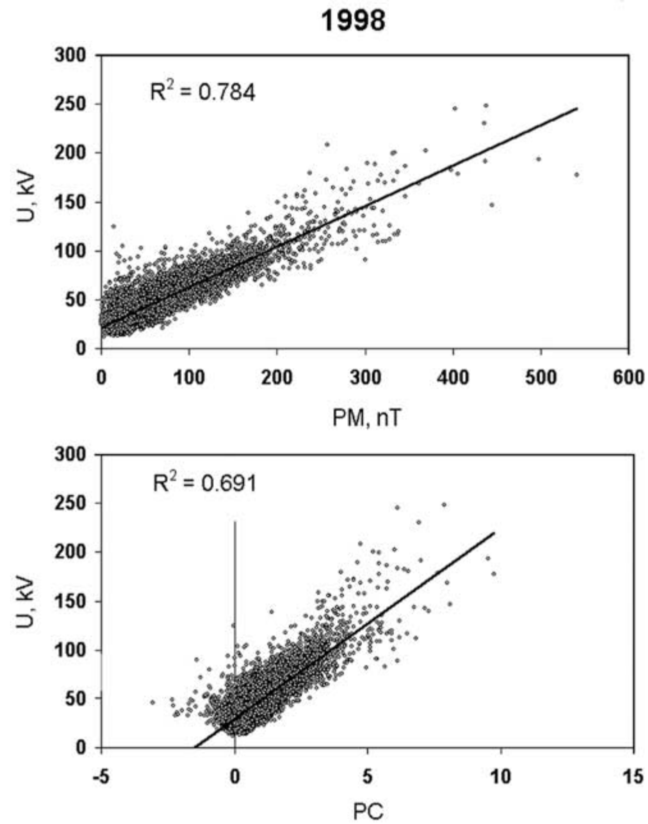

Figure 7. Correlation of hourly mean values of the AMIE cross-polar-cap potential drop, U (kV), with *PM* and *PC* indices for all days of 1998. The AMIE data in this figure and Figures 8 and 9 courtesy of A. Ridley, University of Michigan.

and $JH^{1/2}$. For deriving the predicted values of the CPC voltage, U, and the square root of total hemispheric Joule heating, $JH^{1/2}$, we used the following simple prediction formulas:

$$U_{predict}(\mathrm{kV}) = 15 + 0.28(PM + 9F^*) \tag{15}$$

$$\left[JH_{predict}(\mathrm{GW})\right]^{1/2} = [0.9 + 0.046(PM + 9F^*)] \tag{16}$$

where *PM* index is measured in nT and F^* is the dimensionless coupling function derived from (14). These formulas were found as a linear best fit, optimized to express the real CPC voltage and Joule heating values as functions of the *PM* index and F^* function. The capability of *PM* index in indicating these parameters has been already shown in the correlations in Figure 7 and 8. Using not only *PM* index but also the F^* function allows to provide a more precious prediction than that from using only the *PM* index. The coefficients in these formulas were found to provide the best correlation between predicted and measured values of CPC voltage and *JH*. As shown in Figure 9, the obtained formulas provide a good proxy to the CPC voltage and Joule heating, which may be predicted with a high reliability from *PM* index and upstream solar wind data, which are available in a near-real time.

7. Conclusions

[38] Prediction of geomagnetic activity and related events in the geospace environment is an important task of space weather program. Prediction reliability is dependent on a prediction method and elements included in prediction scheme. Two main elements are an appropriate geomagnetic activity index and an appropriate coupling function (the combination of solar wind parameters providing the best correlation between upstream solar wind data and geomagnetic activity). A reasonable choice of these elements is crucial for any reliable prediction model.

[39] The *PM* index, similarly to the existing *PC* index, was computed from magnetic field measurements from the near-pole geomagnetic observatories, and it shows an integral magnetic effect from ionospheric and remote field-aligned currents, which contribute to the magnetic field variations at these observatories. In distinction from

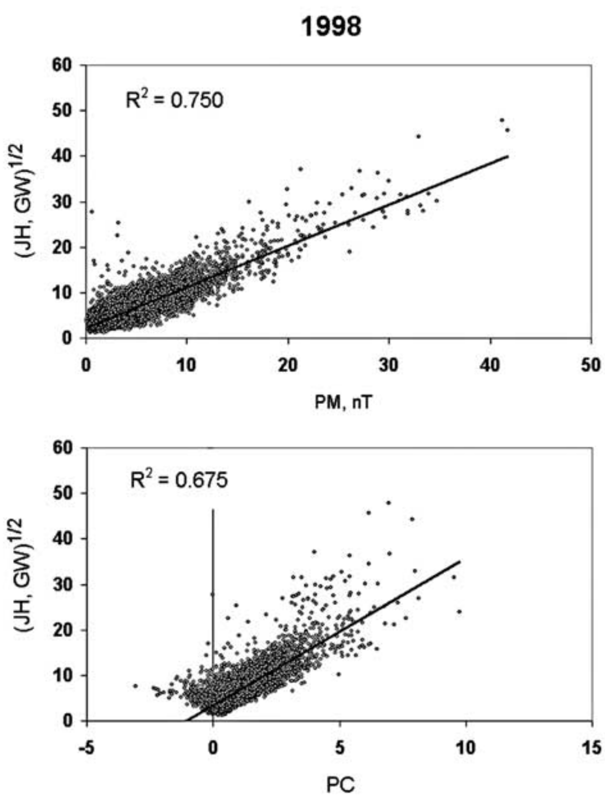

Figure 8. Correlation of hourly mean values of AMIE Joule heating, $JH^{1/2}$, with *PM* and *PC* indices for all days of 1998.

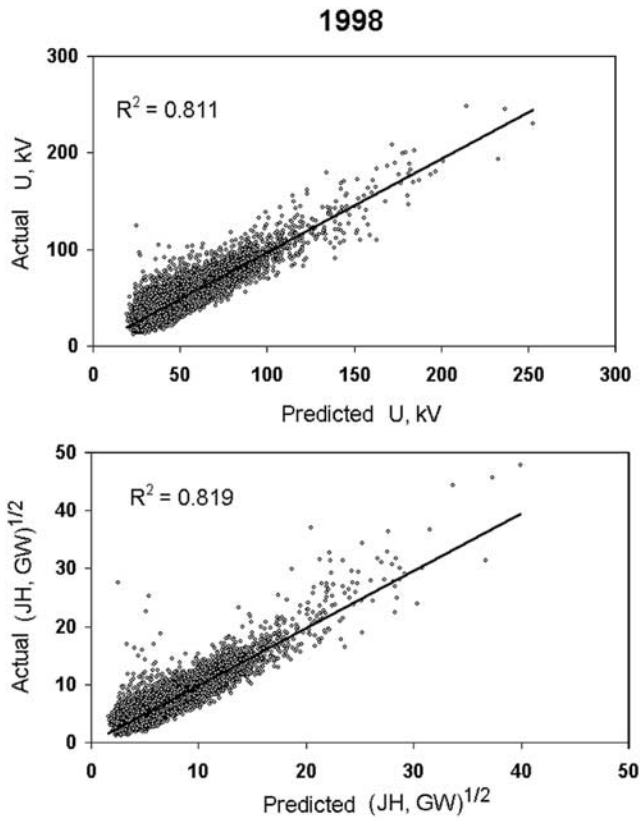

Figure 9. Correlation of the actual (AMIE) and predicted hourly mean values of the cross-polar-cap (CPC) voltage and $JH^{1/2}$ for all days of 1998.

PC index, the *PM* index was developed with using a more advanced method for its computing. In this study, we considered *PM* index computed only in the Northern Hemisphere.

[40] A main distinction of the *PM* index from the existing *PC* index consists in accounting for the contribution from the transpolar equivalent ionospheric current to geomagnetic activity and related events even when this transpolar current is considerably deviated from its average direction. This leads to a significant increase in the correlation between *PM* index and both upstream solar wind/IMF data and related events in geospace environment. As compared with *PC* index, the *PM* index has the following important advantages: (1) It includes the positive values only; (2) It shows significantly smaller seasonal, UT, and solar cycle variations than the *PC* index; (3) It shows a more stable and significantly better correlation with both upstream solar wind/IMF data and related events in the Earth's magnetosphere and ionosphere.

[41] We tested the *PM* index for 10-year period (1995–2004). The correlation between *PM* index and other indices and events in geospace environment is very high for low solar activity but slightly decreases with increasing solar activity. The yearly averages of the squared correlation coefficients, R^2, for the correlation between *PM* index and the solar wind-geomagnetic activity coupling function, auroral electrojet *AL* index, and *Kp* index for this period are about 0.74, 0.71, and 0.68 (see Table 1), which correspond to the linear correlation coefficients $R \approx 0.86$, 0.84, and 0.82, respectively. These correlation coefficients are significantly higher than those for *PC* index.

[42] Table 1 also shows the squared correlation coefficients for the correlation between *PM* index, cross-polar-cap voltage, and hemispheric Joule heating as computed with AMIE technique for 1998. These squared correlation coefficients for *PM* index versus the cross-polar-cap voltage and hemispheric Joule heating are about 0.76 (that correspond to the linear correlation coefficient $R \approx 0.87$). This correlation also is significantly better than that between *PC* index and these quantities.

[43] Using not only *PM* index but also upstream solar wind/IMF data allows even more improving the reliability of prediction of the cross-polar-cap voltage and Joule heating. In this case, the squared correlation coefficient between the actual and predicted values of these two parameters for 1998 reaches $\sim$0.81, which corresponds to the linear correlation coefficient $R \approx 0.9$ and higher.

[44] Thus, the new polar magnetic index of geomagnetic activity provides a significant increase in the reliability of forecasting geomagnetic activity and such key parameters as cross-polar-cap voltage and total Joule heating in high-latitude ionosphere, which play an important role in the development of geomagnetic disturbances and other events in the Earth's magnetosphere and widely used as the key input parameters in modeling ionospheric, ionospheric, and thermospheric processes.

[45] **Acknowledgments.** We are grateful to Aaron Ridley for kind providing us with data on cross-polar-cap potential drop and hemispheric Joule heating in the Northern Hemisphere computed with AMIE technique and Arjun Tan for fruitful collaboration. We also gratefully acknowledge invaluable efforts of the GSFC staff, the National Geophysical Data Center, Danish Meteorological Institute, and World Data Center, Kyoto, Japan in providing solar wind data, geomagnetic activity indices, and data from geomagnetic observatories. This research was performed while Wladislaw Lyatsky held a NASA Senior Postdoctoral Program appointment at

Table 1. Average Values of the Squared Correlation Coefficient, R^2, for the Correlation Between *PM*/*PC* Indices and the Five Parameters: the F^* Solar Wind Coupling Function, *AL* Index, *Kp* Index to the 3/2 Power, Cross-Polar-Cap Voltage, *U*, and Hemispheric Joule Heating, $JH^{1/2}$

	Averages Over 1995–2004			Average for 1998	
	Versus F^*	Versus *AL*	Versus $Kp^{3/2}$	Versus *U*	Versus $JH^{1/2}$
PM	0.74	0.71	0.68	0.78	0.75
PC	0.69	0.66	0.61	0.69	0.67

NASA/MSFC. Funding in support of this study was provided by NASA HQ POLAR project, and NASA LWS program, and partially from the NASA grant NAG5–11995.

References

Akasofu, S.-I. (1981), Energy coupling between the solar wind and the magnetosphere, *Space Sci. Rev.*, *28*, 121–190, doi:10.1007/BF00218810.

Ballatore, P., and C. G. Maclennan (1999), Significance of the high-latitude geomagnetic index AES-80: Comparison with the *PC* index, *Earth Planets Space*, *51*, 425–430.

Borovsky, J. E., and H. O. Funsten (2003), Role of solar wind turbulence in the coupling of the solar wind to the Earth's magnetosphere, *J. Geophys. Res.*, *108*(A6), 1246, doi:10.1029/2002JA009601.

Chun, F. K., et al. (1999), Polar cap index as a proxy for hemispheric Joule heating, *Geophys. Res. Lett.*, *26*, 1101–1104, doi:10.1029/1999GL900196.

Chun, F. K., et al. (2002), Joule heating patterns as a function of polar cap index, *J. Geophys. Res.*, *107*(A7), 1119, doi:10.1029/2001JA000246.

Cliver, E. W., Y. Kamide, and A. G. Ling (2000), Mountains versus valleys: Semiannual variation of geomagnetic activity, *J. Geophys. Res.*, *105*, 2413–2424, doi:10.1029/1999JA900439.

Huang, C.-S. (2005), Variations of polar cap index in response to solar wind changes and magnetospheric substorms, *J. Geophys. Res.*, *110*, A01203, doi:10.1029/2004JA010616.

Kan, J. R., and L. C. Lee (1979), Energy coupling function and solar wind-magnetosphere dynamo, *Geophys. Res. Lett.*, *6*, 577–580, doi:10.1029/GL006i007p00577.

Khazanov, G. V., M. W. Liemohn, T. S. Newman, M.-C. Fok, and R. W. Spiro (2003), Self-consistent magnetosphere-ionosphere coupling: Theoretical studies, *J. Geophys. Res.*, *108*(A3), 1122, doi:10.1029/2002JA009624.

Knipp, D., W. Tobiska, and B. Emery (2004), Direct and indirect thermospheric heating sources for solar cycles 21–23, *Sol. Phys.*, *224*(1–2), 495–505, doi:10.1007/s11207-005-6393-4.

Lu, G., et al. (1995), Magnetosphere-ionosphere-thermosphere coupling: Effect of neutral winds on energy transfer and field-aligned current, *J. Geophys. Res.*, *100*, 19,643–19,659, doi:10.1029/95JA00766.

Lyatsky, W., P. T. Newell, and A. M. Hamza (2001), Solar illumination as cause of the equinoctial preference for geomagnetic activity, *Geophys. Res. Lett.*, *28*, 2353–2356, doi:10.1029/2000GL012803.

Lyatsky, W., A. Tan, and S. Lyatskaya (2006), Monitoring the auroral electrojet from polar cap stations, *J. Geophys. Res.*, *111*, A07202, doi:10.1029/2004JA010989.

Lyatsky, W., S. Lyatskaya, and A. Tan (2007), A coupling function for solar wind effect on geomagnetic activity, *Geophys. Res. Lett.*, *34*, L02107, doi:10.1029/2006GL027666.

Mansurov, S. M. (1981), Characteristics of magnetic disturbances produced by the IMF in the southern polar cap, *Geomagn. Aeron.*, *21*, 428.

Mayaud, P. N. (1980), *Derivation, Meaning, and Use of Geomagnetic Indices*, *Geophys. Monogr. Ser.*, vol. *22*, AGU, Washington, D.C.

McHarg, M., et al. (2005), High-latitude Joule heating response to IMF inputs, *J. Geophys. Res.*, *110*, A08309, doi:10.1029/2004JA010949.

Perreault, P., and S.-I. Akasofu (1978), A study of geomagnetic storms, *Geophys. J. R. Astron. Soc.*, *54*, 547–573.

Richmond, A. D., and Y. Kamide (1988), Mapping electrodynamic features of the high-latitude ionosphere from localized observations: Technique, *J. Geophys. Res.*, *93*, 5741–5759, doi:10.1029/JA093iA06p05741.

Ridley, A. J., and E. A. Kihn (2004), Polar cap index comparisons with AMIE cross-polar-cap potential, electric field, and polar cap area, *Geophys. Res. Lett.*, *31*, L07801, doi:10.1029/2003GL019113.

Rostoker, G. (1972), Geomagnetic indices, *Rev. Geophys. Space Phys.*, *10*, 935–950, doi:10.1029/RG010i004p00935.

Svalgaard, L. (1973), Polar cap magnetic variations and their relationship with the interplanetary magnetic field structure, *J. Geophys. Res.*, *78*, 2064–2078, doi:10.1029/JA078i013p02064.

Troshichev, O. A., A. Janzhura, and P. Stauning (2006), Unified PCN and PCS indices: Method of calculation, physical sense, and dependence on the IMF azimuthal and northern components, *J. Geophys. Res.*, *111*, A05208, doi:10.1029/2005JA011402.

Tsurutani, B. T., and W. D. Gonzalez (1995), The efficiency of "viscous interaction" between the solar wind and the magnetosphere during intense northward IMF events, *Geophys. Res. Lett.*, *22*, 663–666, doi:10.1029/95GL00205.

Weimer, D. R. (2005), Improved ionospheric electrodynamic models and application to calculating Joule heating rates, *J. Geophys. Res.*, *110*, A05306, doi:10.1029/2004JA010884.

G. V. Khazanov and W. Lyatsky, Space Plasma Group, NASA Marshall Space Flight Center, 320 Sparkman Drive, Huntsville, AL 35805, USA. (lyatsky@cspar.uah.edu)